DOI: 10.7860/JCDR/2024/68831.19225

Original Article

Ophthalmology Section

Morphological Changes of Corneal Keratocytes following Surface Ablation Laser Surgery: An Observational Study from the United Kingdom

DAPHNÉ GUNNESS[1], INDRAJIT BANERJEE[2], JARED ROBINSON[3], TEELUCK KUMAR GUNNESS[4]

ABSTRACT

Introduction: Laser Subepithelial Keratomileusis (LASEK) is a type of surface ablation laser surgery that offers a solution to patients for correcting their ametropia. In rare instances, LASEK has been associated with complications such as the development of postoperative haze, infection, and poor visual outcomes. Imaging features detected within the patient's cornea using In-Vivo Confocal Microscopy (IVCM) have aided in identifying the cellular basis of complications like these.

Aim: To observe and describe the morphological changes seen on IVCM in patients following LASEK surgery.

Materials and Methods: This observational study aimed to assess the quantity and morphology of anterior and posterior keratocytes in adults aged 18 years and older. Five participants (9 eyes) who presented for follow-up appointments following LASEK surgery at Manchester Royal Eye Hospital (MREH), United Kingdom, from July to December 2018 were recruited for the study. The cell counts of the anterior and posterior keratocytes were calculated using the Heidelberg Eye Explorer software. The images were analysed with the Image J program (National Institutes of Health, Bethesda, USA). Nerve fibers were assessed using the ACCMetrics program (University of Manchester, UK). The t-test was used to establish the statistical association between variables.

Results: Morphological changes, such as zones of hyper-reflectivity beneath the epithelium, were observed in all the recruited participants. Immune cells and sub-basal nerve abnormalities were detected in several participants. The number of keratocytes in the anterior stroma of all the participants was found to be much lower compared to that of the control. Only participant number 3 had a greater number of keratocytes in the anterior stromal layer (454 and 514 cells/mm^2) compared to the other participants, who had a cell count ranging between 156 to 262 cells/mm^2.

Conclusion: It is evident that visible changes are noted both quantitatively and morphologically in both the anterior and posterior keratocytes postoperatively. More research is required with larger controlled studies to investigate the IVCM imaging biomarkers and morphological features that represent the wound healing process and the factors influencing visual outcomes, ensuring that postoperative complications can be minimised.

Keywords: Laser therapy, Operative, Ophthalmologic surgical procedures, Refractive errors, Refractive surgical procedures

INTRODUCTION

Ametropia is a common ophthalmological condition resulting from abnormal refraction within the eye, which can cause visual impairment. The World Health Organisation (WHO) estimates that refractive errors causes visual impairment in 153 million people globally [1,2]. The four main types of ametropia are myopia (short-sightedness), hypermetropia (long-sightedness), astigmatism, and presbyopia. The most frequent among these is myopia (also known as near-sightedness) [3,4]. The use of spectacles is both the oldest and the most popular method of correction [5]. The second most common treatment modality is contact lenses, which, in their own right, improve the patients' mobility and sporting capabilities but carry inherent risks of infection. If not used properly, contact lenses may damage the cornea. The use of contact lenses also comes with a learning curve, with many patients aborting the process early on due to the difficult trial period [6].

A surgical treatment modality is LASEK, which is a relatively recent and popular type of surface ablation laser surgery offering a solution to patients willing to correct their ametropia by changing the shape of their cornea. LASEK surgery was developed in the 1980s and has become a popular method for the correction of such refractive errors, with the aim of spectacle and contact lens independence [7]. As with all the modalities of treatment, LASEK has both advantages and disadvantages. In the majority of cases, the procedure is painless, rapid, and highly effective with excellent results, often allowing patients to be discharged on the same day of the procedure. However, there are cases where complications occur, and as a result, the vision of the patient may be further compromised. In rare instances, LASEK can be associated with complications such as the development of postoperative haze that can contribute to a poor visual outcome [7]. Many studies have been conducted to understand the long-term effect of such procedures on the cornea, most prominently the morphological changes evident in the corneal keratocytes [7-9].

A better understanding of the postoperative morphological impacts of LASEK will provide insight into how to reduce postoperative complications. There is a lack in the available literature on the postoperative morphological changes noted after such LASEK procedures, making the novelty of this study and its future implications valuable and demanding further investigation and attention. This research aimed to observe corneal cellular changes in-vivo in the stroma of patients who had undergone LASEK surgery through the use of IVCM. The study includes the analysis of keratocyte cellular density, the Sub-Basal nerve Plexus (SBP), and the description of abnormal findings, such as the presence of dendritiform cells or zones of scar tissue.

MATERIALS AND METHODS

This observational study aimed to assess the quantity and morphology of anterior and posterior keratocytes following LASEK surgery conducted at MREH, United Kingdom, from July to December 2018. The study was reviewed and approved by the North East York Research Committee (NREC) as part of a broader project entitled "Corneal imaging uses to monitor corneal disease and treatment" with approval no. (Reference: 15/NE/0363). All participants provided informed consent. This research was conducted based on the Ethical Principles for Medical Research involving Human Subjects guidelines as per the Declaration of Helsinki.

Inclusion criteria: Adults aged 18 years and older who had undergone LASEK surgery for myopia or astigmatism at MREH were recruited. Participants were required to read and understand the provided patient information sheet, ask questions to the researcher, and provide consent by signing the informed consent document. One healthy adult volunteer served as a control.

Exclusion criteria: Patients with ocular infections, painful eyes, or previous intraocular injuries. Children were not included in the study, and there was no limit to the timeframe between the LASEK surgery and assessment.

Sample size: Five participants (nine eyes) who had undergone LASEK surgery for myopia or astigmatism from July to December 2018 at MREH, United Kingdom, were recruited for follow-up appointments. The primary treatment for refractive errors is typically through the use of spectacles and contact lenses, with LASEK surgery being a relatively recent and rare surgical treatment modality.

Methodology and Parameters Studied

LASEK Surgery: Patients in this study underwent the same LASEK surgery technique. The eye was anesthetised with preservative-free Minims proxymetacaine 0.5% eyedrops (Bausch and Lomb, UK). A trephine was used to mark a circular area with a diameter of 9 mm for debriding the corneal epithelium. A 20% ethanol solution was topically applied to this area for 20 to 30 seconds, and the loosened epithelial flap was then elevated. Subsequently, the underlying stroma was ablated using the ALEGRETTO Wave Excimer Laser (WaveLight Laser Technologie AG, Germany). The Heidelberg Retina Tomograph 3 (HRT 3), a laser scanning in-vivo confocal microscope (Heidelberg Engineering, Germany), was utilised to obtain high-resolution images of the corneal layers. Images were obtained using the volume scan mode. Each volume scan consisted of a z-stack of 40 successive images automatically acquired with a ±2 µm distance between consecutive images. Images were taken at various depths of the entire cornea, including the epithelium, anterior stroma, posterior stroma, and endothelium.

Image analysis: Images were analysed both quantitatively and qualitatively. The cell counts of the anterior and posterior keratocytes were calculated using the Heidelberg Eye Explorer software. The images were analysed with the Image J program (National Institutes of Health, Bethesda, USA). Nerve fibers were assessed using the ACCMetrics program (University of Manchester, UK).

STATISTICAL ANALYSIS

The data was analysed using Statistical Package for Social Sciences (SPSS) software for Windows version 26.0. The t-test was used to establish the statistical association between variables. A p-value <0.05 was considered statistically significant.

RESULTS

Out of the six patients, five had undergone LASEK surgery and were considered cases. Confocal images from the eyes of a 21-year-old male volunteer who hadn't undergone LASEK surgery were taken as a further control [Table/Fig-1].

Participant	Age (years)/ Gender	Time post-LASEK	Case/ Control	Outcome
1	69/F	Right eye: 9 months; Left eye: 7 months	Case	Both eyes: Good visual outcome
2	26/M	Both eyes: 4 months	Case	Right eye: Subepithelial haze and reduced visual acuity Left eye: Good visual outcome
3	31/M	Both eyes: 5 months	Case	Both eyes: Good visual outcome
4	49/M	Both eyes: 7 years	Case	Right eye: Very poor visual acuity Left eye: Good visual outcome
5	24/M	Right eye: 8 months	Case	Both eyes: Good visual outcome
6	21/M	Both eyes (Control: No LASEK)	Control	Not applicable (control participant)

[Table/Fig-1]: Demographic data for each participant.

Control: The epithelium was composed of small polygonal and regular cells. On IVCM, they appeared as dark cells surrounded by hyper-reflective borders. The SBP was situated at the level of the Bowman's membrane. Nerves appeared as thin longitudinal hyper-reflective structures. Keratocyte nuclei were visible as bean-shaped hyper-reflective structures, and their processes were normally transparent (thus invisible on IVCM). The last visible layer was the endothelium (Descemet's membrane, which sits just above the endothelium, is not visible on IVCM). The endothelium was composed of regular bright polygonal cells. The IVCM images from the control showing the normal layers of the cornea are displayed in [Table/Fig-2].

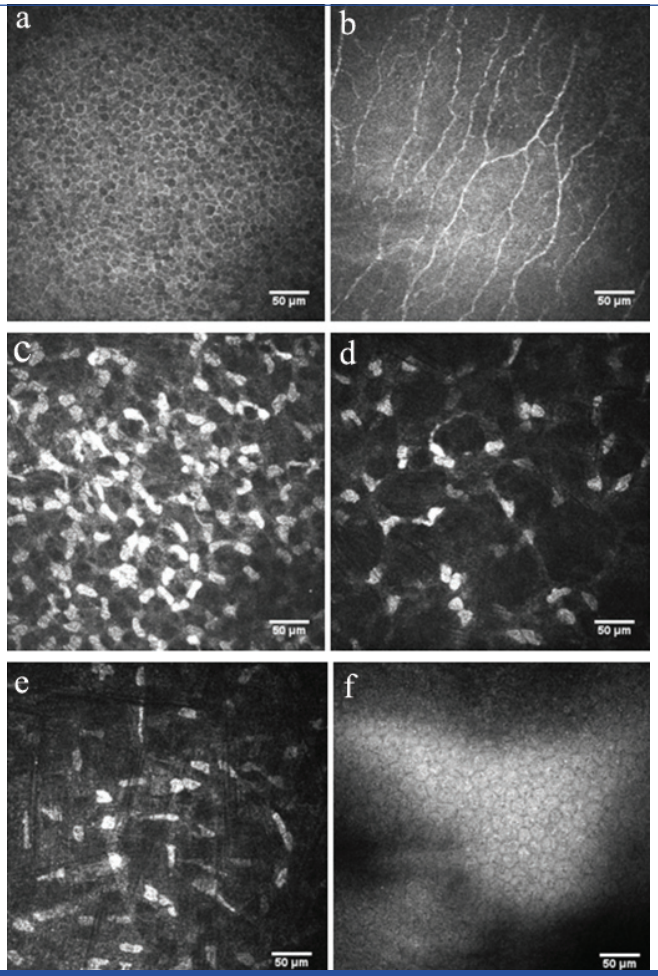

[Table/Fig-2]: IVCM of layers of cornea from control. a) Epithelium; b) Sub-basal nerve Plexus (SBP); c) Anterior stroma; d) Middle stroma; e) Posterior stroma; f) Endothelium.

Image analysis: The IVCM images from participant one's right and left eyes are shown in [Table/Fig-3,4], respectively.

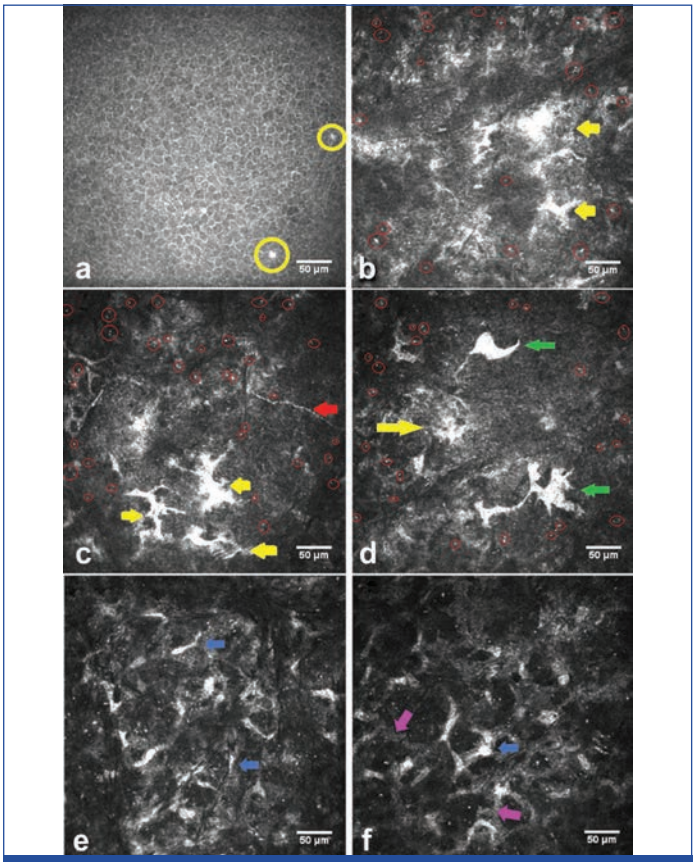

[Table/Fig-3]: IVCM of the right eye of participant 1. a) Epithelium; b-d) Below epithelium; e-f) Anterior Stroma. Yellow arrow: zones of hyper-reflectivity, hypothesized to be dendritiform cells. Yellow circles: immune cell subtypes. Red circles: granules. Green arrows: unidentified hyper-reflective zones. Red arrow: beaded sub-basal nerve. Blue arrows: keratocytes cell bodies.

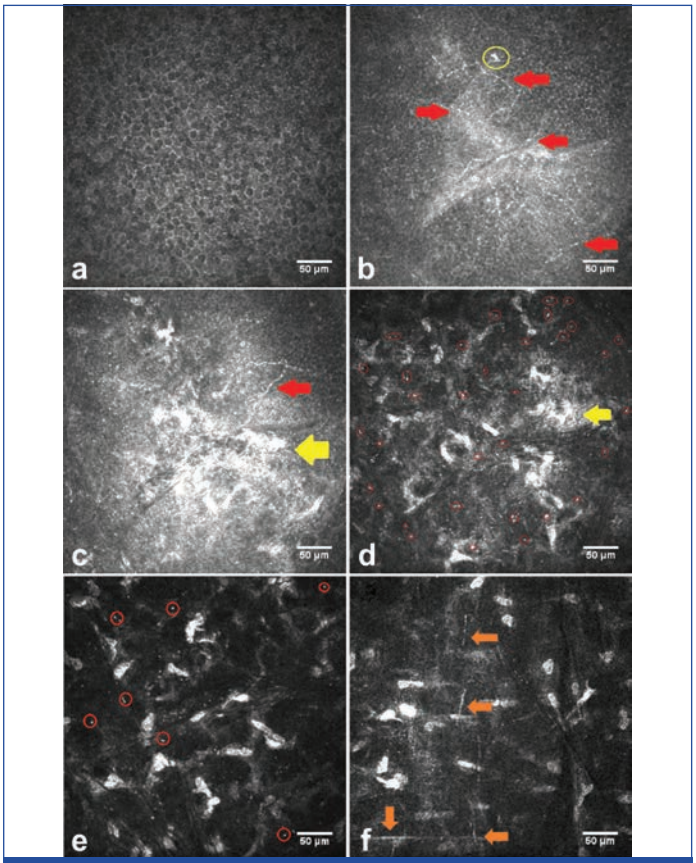

[Table/Fig-4]: IVCM of the left eye of participant 1. a) Epithelium; b) Epithelium and Sub-basal nerve Plexus (SBP); c) Below epithelium; d) Anterior stroma; e) Mid-Stroma; f) Posterior stroma. Yellow arrow: zones of hyper-reflectivity. Red arrows: sub-basal nerves. Yellow and red circles: immune cell subtypes. Orange arrows: spindle-like lines.

Participant-1 had undergone the LASEK procedure in both eyes. Overall, the basal layer of the epithelium of the right eye appeared to be normal [Table/Fig-3a]. There were two zones of hyper-reflectivity within the deeper sections of the epithelium extending into the anterior stroma (yellow arrows), which would be consistent with that of a dendritiform cell type. Smaller cells were also present in [Table/Fig-3] shown in the yellow circles and measuring less than 10 µm. It was hypothesised that these could all be subtypes of immune cells. The epithelium of the left eye of participant-1 is illustrated in [Table/Fig-4]. There was no remarkable difference between this epithelium and the control. An extensive number of granules were found in both eyes of participant 1 (red circles, [Table/Fig-3,4]).

Participant-2 had undergone the LASEK procedure most recently in both eyes (four months prior to the study). It is important to note that subepithelial haze was noticed in his right eye on slit-lamp biomicroscopy on the day of the assessment. The patient's visual acuity was better in his left eye (-0.10 on LogMar) compared to his right eye (+0.1 on LogMar) on the day of the assessment. Zones of poorly defined and opaque hyper-reflective tissue were detectable in both eyes (yellow arrows, [Table/Fig-5,6]).

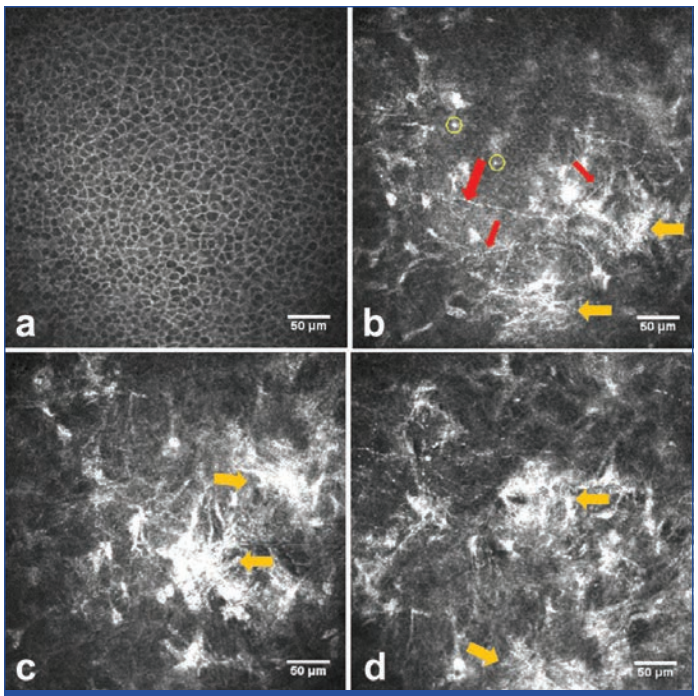

[Table/Fig-5]: IVCM of the right eye of participant 2. a) Epithelium; b) Sub-basal nerve plexus (SBP); c and d) Below epithelium. Yellow circles: immune cells. Yellow arrows: zones of scar tissue. Red arrow: beaded sub-basal nerve.

Participant 3 had undergone LASEK in both eyes five months prior to the day of assessment. The epithelium in the left eye and right eye of participant three showed no abnormalities ([Table/Fig-7a,8a]). Zones of poorly defined and opaque hyper-reflective tissue were detectable, as well as dendritiform cells ([Table/Fig-7,8], white arrows).

Participant 4 had undergone LASEK surgery in both eyes seven years prior to the assessment. Following surgery, he developed complications, including epithelial defects, formation of an epithelial cyst, and subsequent scarring. The visual acuity in his right eye was at logMAR +0.84 at the time of assessment and -0.08 for his left eye. IVCM imaging in [Table/Fig-9] shows a normal epithelial cell appearance but with the presence of small dendritiform cells (yellow circles in 'a'). [Table/Fig-9b] shows swathes of hyper-reflective material following Bowman's membrane collagen fibrils (orange arrows) and prominent corneal nerves (red arrows [Table/Fig-9b,c]). Further linear structures were noted in the stroma (orange arrows in 'd') that may represent corneal nerve branches. [Table/Fig-10c] shows prominent, tortuous, and beaded corneal nerve fibers in the basal corneal plexus (red arrows) with associated dendritiform

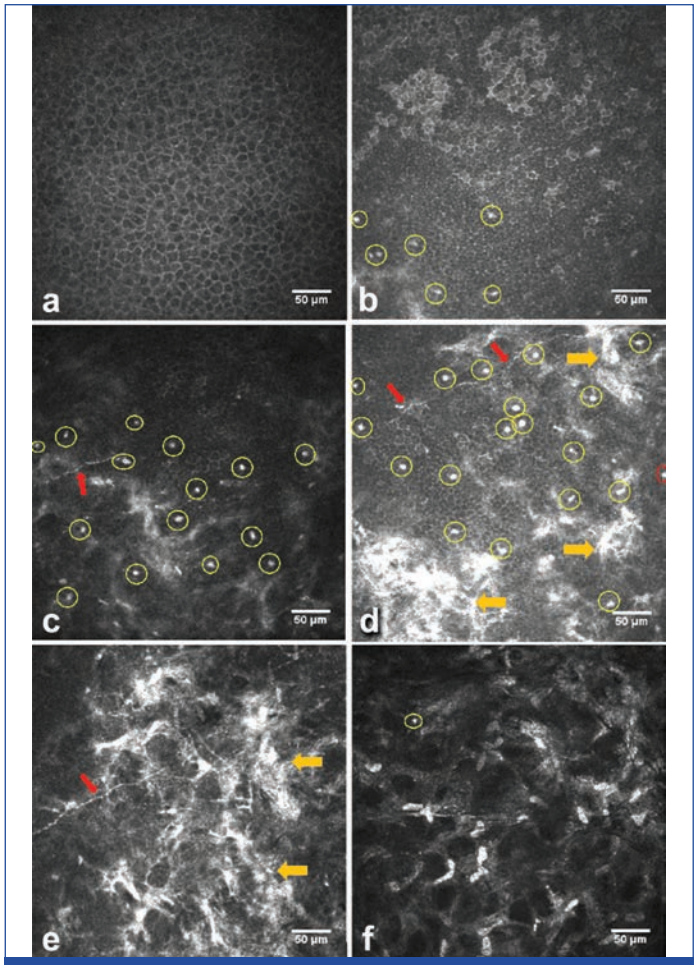

[Table/Fig-6]: IVCM of the left eye of participant 2. a-d) Epithelium; e) Below epithelium; f) Anterior Stroma. Yellow circles: immune cells. Red arrows: sub-basal nerves; Yellow arrows: zones of hyper-reflectivity.

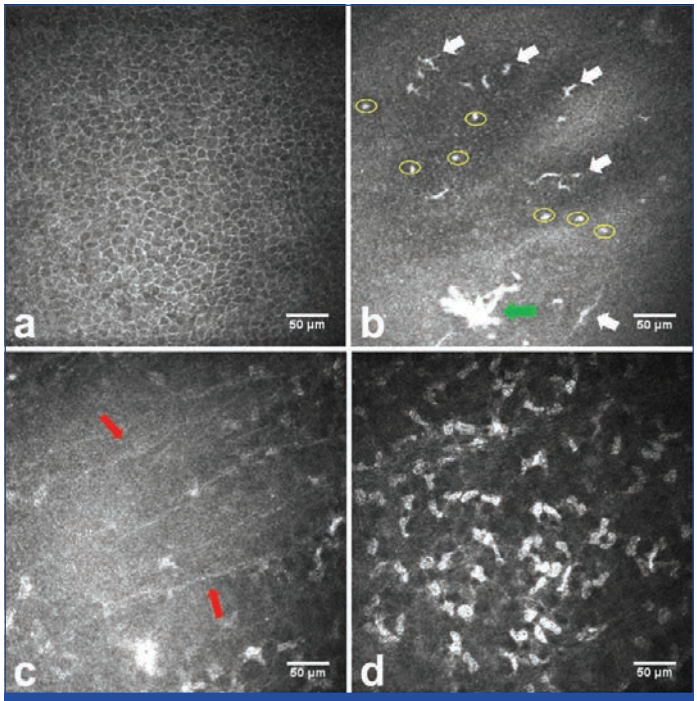

[Table/Fig-7]: IVCM of the right eye of participant 3. a) Epithelium; b) Below epithelium; c) Sub-Basal nerve Plexus (SBP); d) Anterior stroma. White arrows: dendritiform cells. Yellow circles: immune cells. Red arrows: sub-basal nerves. Green arrow: zone of hyper-reflectivity.

small cells (yellow circles), along with prominent keratocyte nuclei in [Table/Fig-10d] (yellow arrow) signifying an activated keratocyte phenotype in the left eye [Table/Fig-9,10].

Participant 5 had undergone the laser surgery eight months on the right eye prior to being assessed for this study. Only the right eye could be assessed due to the participant's time constraints.

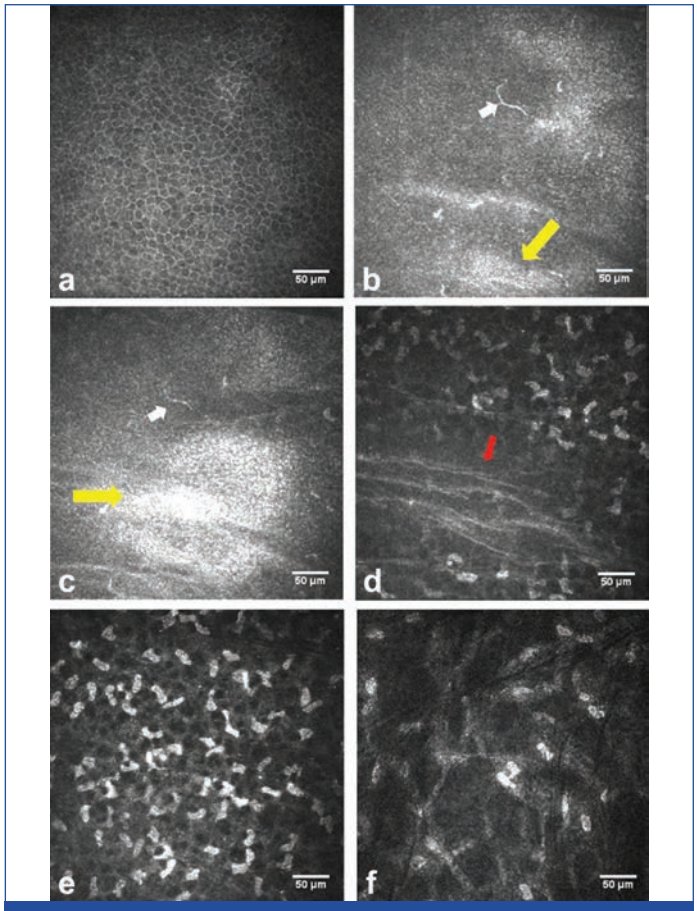

[Table/Fig-8]: IVCM of the left eye of participant 3. a) Epithelium; b,c) Below epithelium. d) Sub-Basal nerve Plexus (SBP); e) Anterior stroma; f) Mid-Stroma; g) Posterior Stroma. White arrows: dendritiform cells. Yellow arrows: zones of hyper-reflectivity. Red arrows: sub-basal nerves.

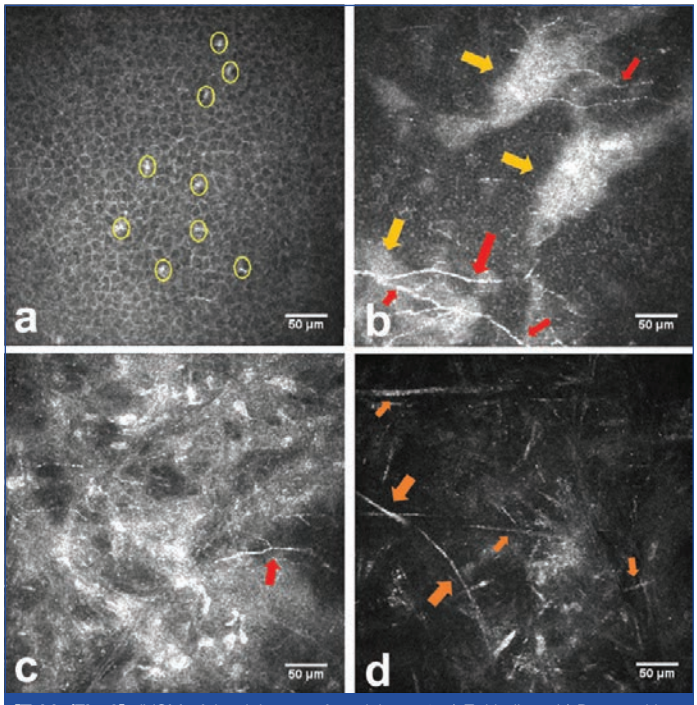

[Table/Fig-9]: IVCM of the right eye of participant 4. a) Epithelium; b) Deep epithelium; c,d) Anterior stroma. Yellow circles: immune cells, dendritiform appearance. Yellow arrows: zones of scar tissue. Red arrows: sub-basal nerves. Orange arrows: spindle-like lines.

Zones of poorly defined and opaque hyper-reflective tissue were detectable [Table/Fig-11c]. Corneal nerves appeared beaded and slightly tortuous (red arrows in [Table/Fig-11b]), and small hyper-reflective opacities associated with keratocytes are seen in the red circles in [Table/Fig-11d].

Keratocyte cell count: A variation between the number of cells per square millimeter within the different layers of the stroma of

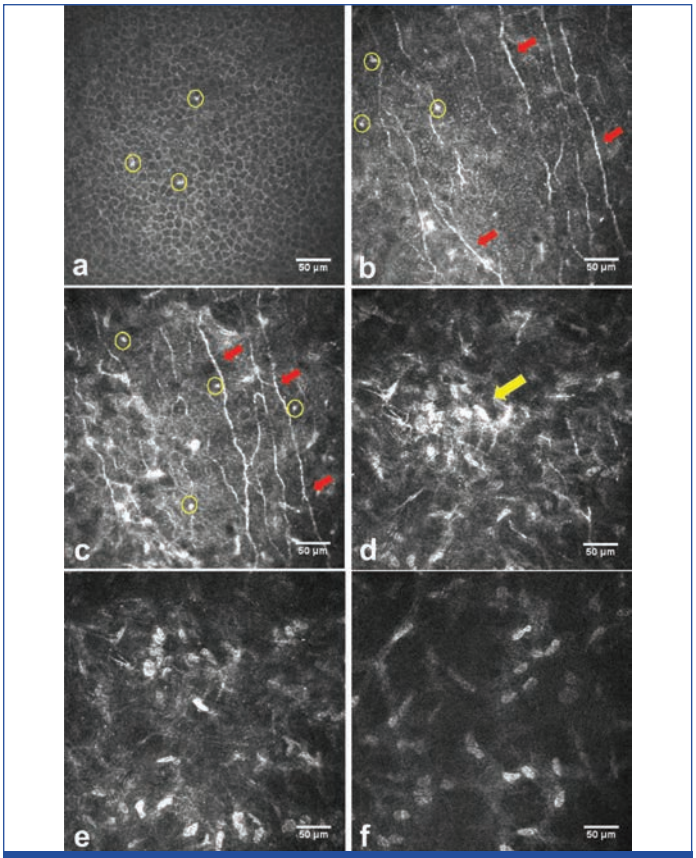

[Table/Fig-10]: IVCM of the left eye of participant 4. a) Epithelium; b,c) Sub-Basal nerve Plexus (SBP); d,e) Anterior stroma; f) Mid-Stroma. Yellow circles: immune cells. Yellow arrows: zones of scar tissue. Red arrows: sub-basal nerves.

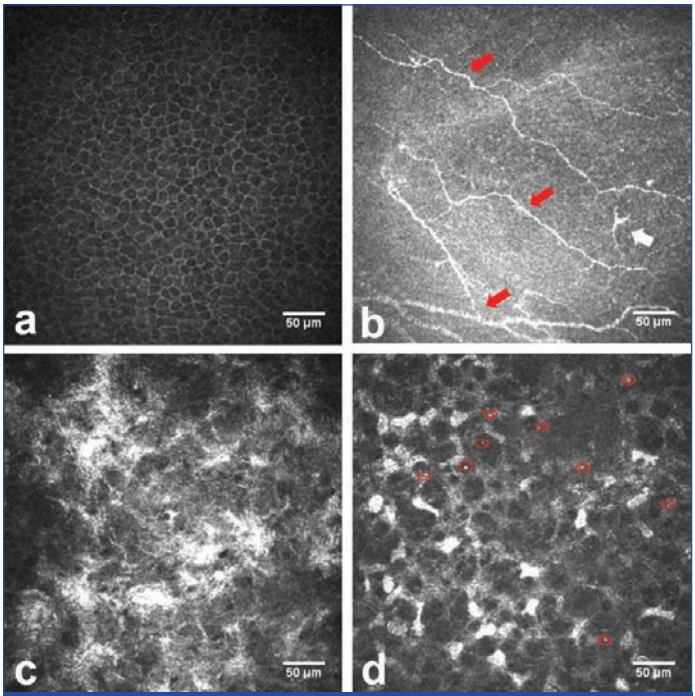

[Table/Fig-11]: IVCM of the right eye of participant 5. a) Epithelium; b) Sub-Basal nerve Plexus (SBP); c) Below epithelium; d) Anterior stroma. Red arrows: sub-basal nerves. White arrows: dendritic cells.

each patient's cornea was observed. A single control cell count was obtained per layer, a t-test was performed in order to determine whether there was a statistically significant difference between the control and the participants' keratocyte cell counts [Table/Fig-12].

The number of keratocytes in the anterior stroma of the participants was lower than that of the control cornea. Only participant number 3 had a greater number of keratocytes in the anterior stromal layer (454 and 514 cells/mm^2) compared to the other participants, who had a cell count which varied from 156 to 262 cells/mm^2. It is interesting to note that the differences between the posterior keratocyte cell count

Eye	Keratocytes anterior stroma (cells/mm^2)	Keratocytes middle stroma (200-300 µm deep) (cells/mm^2)	Keratocytes posterior stroma (cells/mm^2)
Control	687	225	267
1 OD	200	275	244
1 OS	163	231	175
2 OD	156	250	150
2 OS	246	231	227
3 OD	454	227	168
3 OS	514	212	250
4 OD	176	235	144
4 OS	229	208	196
5 OD	262	218	217
p-value*	0.015*	0.759	0.133

[Table/Fig-12]: Keratocytes cell count.
(The standard deviation SD given by the Heidelberg software varied between ±8 to ±10 cells / mm^2). OD = right; OS = left. t-test was used to establish the statistical association between variables. The p-value was obtained by comparing the keratocytes counts compared to the control. *p-value has been rounded.

of the right and left eyes of the same person are more significant than the differences between different participants. For instance, the posterior keratocyte cell count of participant 3's left eye is 250 cells/mm^2, which is closer to the posterior keratocyte cell count of participant 2's left eye (227 cells/mm^2) compared to participant 3's right eye (168 cells/mm^2).

Nerve fibre assessment using the ACC: Except for the isolated sub-basal nerves mentioned previously, adequate SBP images could not be observed in Participants 1, 2, and 3. This is an important result in itself: either the SBP did not manage to regenerate themselves sufficiently following LASEK surgery, or the scar tissue that formed as a response to the trauma obstructed the visualisation of the corneal basal nerve plexus. The main observation from these results was the increased nerve fiber branching density observed in participant 5. [Table/Fig-13] summarises the nerve analysis obtained from the ACCMetrics software.

Sub-Basal nerve Plexus (SBP)	Control	4OD	4 OS	5 OD
Corneal Nerve Fibre Density (CNFD) (no/mm^2)	37.4976	12.4992	12.4992	31.2480
Corneal Nerve Branch Density (CNBD) (no/mm^2)	24.9984	31.2480	12.4992	56.2464
Corneal Nerve Fibre Length (CNFL) (mm/mm^2)	16.8614	10.2991	15.5985	13.4696
Corneal Nerve Fibre Total Branch Density (CTBD) (no/mm^2)	31.2480	37.4976	43.7472	87.4944
Corneal Nerve Fibre Area (CNFA) (mm^2/mm^2)	0.0070	0.0073	0.0092	0.0093
Corneal Nerve Fibre Width (CNFW) (mm/mm^2)	0.0215	0.0230	0.0264	0.0236

[Table/Fig-13]: Sub-basal nerves analysis.

DISCUSSION

In this study, morphological changes, such as zones of hyper-reflectivity beneath the epithelium, were observed in all recruited participants. Immune cells and sub-basal nerve abnormalities were detected in several participants.

Epithelium and immune cells: The overall morphology of the corneal epithelium observed in this study was consistent with the literature. It was found that one month following surface-ablation refractive surgery, the epithelial cells regain their typical appearance [10,11]. The presence of small, circular, and hyper-reflective cells in the deepest layers of the epithelium was observed in several of the eyes and was hypothesised to be immune in nature. The review by Guthoff RF et al., examined and classified the different types of leukocytes that are visible on IVCM [12]. Dendritiform-

shaped cells and smaller round cells were identified in present study. These cells were likely to be Langerhans Cells (LC), and the smaller cells were likely to be other types of leukocytes. LC manifest as cells with long processes which have a typical spider-like or dendritiform appearance with IVCM [12]. These cells are similar to the ones observed in participant 3. The presence of these cells could indicate an inflammatory reaction, as they appear enlarged compared to the smaller LCs found in the central basal cornea in healthy participants [13]. There was no clear relationship between the presence of dendritiform cells and the participant's visual outcome in this small case study; however, further research is needed to confirm if there is any association.

Zones of scar tissue: Zones of poorly defined and opaque hyper-reflective tissue were detectable in all participants. This was consistent with other research studies that found patients undergoing surface-ablation surgery revealed increased subepithelial reflectivity [10,11]. This result was particularly interesting considering that not all of the participants had clinical haze detectable on slit lamp microscopy or reduced visual acuity (except participant 2). Moilanen JA et al., made a similar observation in their study assessing long-term morphological changes of the cornea five years following Photorefractive Keratectomy (PRK) [14]. More extensive zones of subepithelial hyper-reflectivity were observed in the right eye of participant 2, which appeared to be in Bowman's membrane, and this eye was also noted to have the presence of visible subepithelial corneal haze on slit-lamp microscopy. This participant also presented with reduced visual acuity in this right eye compared to that of the left eye. The morphology of scarring that present study reported in Bowman's membrane may be indicative of hyper-reflective scar tissue and may contribute to the participant's reduced visual acuity.

Keratocyte appearance: Following refractive surgery, keratocytes are "activated" and display a different morphology on IVCM than when they are quiescent [15,16]. In this study, on the IVCM images, enlarged hyper-reflective keratocyte nuclei and cellular processes in the right eye of participant 1, the left eye of participant 2, and the right eye of participant 5 were observed. The presence of keratocyte activation in these IVCM images may indicate prolonged resolution of inflammation in the corneal stroma even months post-LASEK [17-19]. These activated keratocytes or myofibroblasts are believed to express α-Smooth Muscle Actin (α-SMA) and are thought to be responsible for the development of fibrosis and haze following surface-ablation surgery [15]. Møller-Pedersen T et al., reported the presence of these activated keratocytes a week after PRK in the anterior stroma. Only a few of these keratocytes were observed in the posterior stroma of participant 1, who had LASEK seven months prior to the assessment [11]. On the contrary, the vast majority of these activated keratocytes were observed in participant 4, who had surgery seven years before the assessment. To the best of our knowledge, such morphological appearances of activated keratocytes have not previously been reported and have yet to be observed in patients after such a long period post-LASEK. In this participant, the co-occurrence of swathes of hyper-reflective material mimicking collagen lamellae in Bowman's membrane, as well as the activated keratocyte morphology, may have contributed to the poor visual outcome of this patient.

Other morphological changes: The presence of fine hyper-reflective foci <10 microns in diameter on IVCM observed in the study of Møller-Pedersen T et al., who referred to them as "punctate deposits," are believed to be the results of keratocyte apoptosis or necrosis [11]. These granules were also observed in other conditions, such as keratitis [20]. Moreover, it has been noticed that these deposits seem to be present and numerous in IVCM imaging in long-term contact lens wearers [21]. An extensive number of granules were found in both eyes of participant 1, but data was not collected regarding contact lens use prior to the LASEK procedure.

Patel DV and McGhee CN reported the results of 19 studies that had presented their keratocyte cell count results [16]. The results of the keratocyte cell counts vary significantly across the studies and depending on the gender and age range of patients studied. For instance, Popper M et al., reported a normal human anterior keratocyte cell count of 258 cells/mm^2, whereas Pisella PJ et al., obtained an anterior keratocyte cell count of 1060±468 cells/mm^2 [22,23]. Both of these studies examined normal eyes using the white light-based Scanning-Slit Confocal Microscope (SSCM), which has lower resolution than the HRT3 laser scanning IVCM. Similar findings are noted with the present study; however, a lower anterior cell count ranging from 150 to 250 cells/mm^2 was noted in all of the patients barring one.

SBP: Present study detected a greater corneal nerve branch density in participant 5. The SBP of participants 1, 2, and 3 could not be visualised on IVCM because of scar tissue. Further studies are needed with more controls and more participants to determine whether there is a statistically significant difference between the morphological features of the SBP of patients post-LASEK as compared with that of the normal SBP. A prospective study from Darwish T et al., found that, although corneal sensitivity came back to normal three months following laser refractive surgery, the structure of SBP was still abnormal six months following the procedure [24]. It would be interesting and relevant to investigate the link between SBP regeneration following LASEK and the keratocyte cell count, as a study from Kalteniece A et al., demonstrated that corneal nerve damage in diabetic patients is linked to reduced anterior, mid, and posterior keratocytes [25].

One of the strengths of this study lies in its emphasis on real-world applications. By linking morphological changes to surface-ablation laser surgery, this study bridges the gap between theoretical knowledge and practical implications. This connection enhances the study's relevance to ophthalmologists, refractive surgeons, and anyone interested in advancements in laser eye surgery.

Limitation(s)

The study was limited by a relatively small sample size of patients from a hospital in the United Kingdom. A larger multicentric study and a more diverse sample could enhance the generalisability of the results to a broader population.

CONCLUSION(S)

It is evident that visible changes were noted both quantitatively and morphologically in both the anterior and posterior keratocytes postoperatively. More research is required with larger controlled studies in order to investigate the IVCM imaging biomarkers and morphological features that represent the wound healing process and the factors that influence visual outcomes to ensure that postoperative complications can be minimised. A longitudinal study with extended follow-up periods would provide a more comprehensive understanding of these morphological changes over time.

Acknowledgement

The authors wish to thank Dr. Chantal Hillarby, Mr. Arun Brahma, and Dr. Jaya Chidambaram for their invaluable contributions to this study.

REFERENCES

[1] World Health Organization. (n.d.). Blindness and vision impairment: Refractive Errors. World Health Organization. Cited [2023 November 25] Available from: https://www.who.int/news-room/questions-and-answers/item/blindness-and-vision-impairment-refractive-errors.

[2] Shi XY, Ke YF, Jin N, Zhang HM, Wei RH, Li XR. The prevalence of vision impairment and refractive error in 3654 first year students at Tianjin Medical University. Int J Ophthalmol. 2018;11(10):1698-703. Doi: 10.18240/ijo.2018.10.19. PMID: 30364305; PMCID: PMC6192952.

[3] Abdulsalam HO, Muhammad N, Pam V, Oladigbolu KK. Pattern of ametropia, presbyopia, and barriers to the uptake of spectacles in adult patients attending a general hospital in Kaduna State. J West Afr Coll Surg. 2022;12(1):28-33. Doi: 10.4103/jwas.jwas_70_22. Epub 2022 Aug 23. PMID: 36203913; PMCID: PMC9531742.
[4] Schiefer U, Kraus C, Baumbach P, Ungewiß J, Michels R. Refractive errors. Dtsch Arztebl Int. 2016;113(41):693-702. Doi: 10.3238/arztebl.2016.0693. PMID: 27839543; PMCID: PMC5143802.
[5] Ong E, Grice K, Held R, Thorn F, Gwiazda J. Effects of spectacle intervention on the progression of myopia in children. Optom Vis Sci. 1999;76(6):363-69.
[6] Heus P, Verbeek JH, Tikka C. Optical correction of refractive error for preventing and treating eye symptoms in computer users. Cochrane Database Syst Rev. 2018;4(4):CD009877. Doi: 10.1002/14651858.CD009877.pub2. PMID: 29633784; PMCID: PMC6494484.
[7] Taneri S, Zieske JD, Azar DT. Evolution, techniques, clinical outcomes, and pathophysiology of LASEK: Review of the literature. Surv Ophthalmol. 2004;49(6):576-602.
[8] Ambrosio Jr RE, Jardim D, Netto MV, Wilson SE. Management of unsuccessful LASIK surgery. Compr Ophthalmol Update. 2007;8(3):125-41.
[9] Chung A, Brahma A. LASIK eye surgery: Standard and safety issues. Clinical Risk. 2006;12(2):70-73.
[10] Frueh BE, Cadez R, Böhnke M. In-vivo confocal microscopy after photorefractive keratectomy in humans. A prospective, long-term study. Arch Ophthalmol. 1998;116(11):1425-31. Doi: 10.1001/archopht.116.11.1425. PMID: 9823340.
[11] Møller-Pedersen T, Vogel M, Li HF, Petroll WM, Cavanagh HD, Jester JV. Quantification of stromal thinning, epithelial thickness, and corneal haze after photorefractive keratectomy using in-vivo confocal microscopy. Ophthalmology. 1997;104(3):360-68. Doi: 10.1016/s0161-6420(97)30307-8. PMID: 9082257.
[12] Guthoff RF, Zhivov A, Stachs O. In-vivo confocal microscopy, an inner vision of the cornea- A major review. Clin Exp Ophthalmol. 2009;37(1):100-17. Doi: 10.1111/j.1442-9071.2009.02016.x.
[13] Zhivov A, Stave J, Vollmar B, Guthoff R. In-vivo confocal microscopic evaluation of Langerhans cell density and distribution in the normal human corneal epithelium. Graefes Arch Clin Exp Ophthalmol. 2005;243(10):1056-61. Doi: 10.1007/s00417-004-1075-8. Epub 2005 Oct 20. PMID: 15856272.
[14] Moilanen JA, Vesaluoma MH, Müller LJ, Tervo TM. Long-term corneal morphology after PRK by in-vivo confocal microscopy. Invest Ophthalmol Vis Sci. 2003;44(3):1064-69. Doi: 10.1167/iovs.02-0247. PMID: 12601030.
[15] Zhivov A, Stachs O, Kraak R, Guthoff R. Zelluläre Lasermikroskopie zur Detektion von Infiltraten und Ulzera der Hornhaut [Cellular laser microscopy of corneal ulcer and infiltrate]. Klin Monbl Augenheilkd. 2008;225(1):86-90. German. Doi: 10.1055/s-2008-1027130. PMID: 18236377.
[16] Patel DV, McGhee CN. Contemporary in-vivo confocal microscopy of the living human cornea using white light and laser scanning techniques: A major review. Clin Exp Ophthalmol. 2007;35(1):71-88. Doi: 10.1111/j.1442-9071.2007.01423.x. PMID: 17300580.
[17] Patel DV, McGhee CN. Quantitative analysis of in-vivo confocal microscopy images: A review. Surv Ophthalmol. 2013;58(5):466-75. Doi: 10.1016/j.survophthal.2012.12.003. Epub 2013 Feb 28. PMID: 23453401.
[18] McLaren JW, Bourne WM, Patel SV. Automated assessment of keratocyte density in stromal images from the ConfoScan 4 confocal microscope. Invest Ophthalmol Vis Sci. 2010;51(4):1918-26. Doi: 10.1167/iovs.09-4186. Epub 2009 Nov 5. PMID: 19892869; PMCID: PMC2868412.
[19] McLaren JW, Patel SV, Nau CB, Bourne WM. Automated assessment of keratocyte density in clinical confocal microscopy of the corneal stroma. J Microsc. 2008;229(Pt 1):21-31. Doi: 10.1111/j.1365-2818.2007.01870.x. PMID: 18173641; PMCID: PMC2700340.
[20] Chidambaram JD, Prajna NV, Palepu S, Lanjewar S, Shah M, Elakkiya S, et al. In-vivo confocal microscopy cellular features of host and organism in bacterial, fungal, and acanthamoeba keratitis. Am J Ophthalmol. 2019;190:24-33. Doi: 10.1016/j.ajo.2018.03.010. Epub 2018 Mar 14. PMID: 29550185; PMCID: PMC5972002.
[21] Villani E, Baudouin C, Efron N, Hamrah P, Kojima T, Patel SV, et al. In-vivo confocal microscopy of the ocular surface: From bench to bedside. Curr Eye Res. 2014;39(3):213-31. Doi: 10.3109/02713683.2013.842592. Epub 2013 Nov 11. PMID: 24215436; PMCID: PMC3960287.
[22] Popper M, Morgado AM, Quadrado MJ, Van Best JA. Corneal cell density measurement in-vivo by scanning slit confocal microscopy: Method and validation. Ophthalmic Res. 2004;36(5):270-76. Doi: 10.1159/000081207. PMID: 15583433
[23] Pisella PJ, Auzerie O, Bokobza Y, Debbasch C, Baudouin C. Evaluation of corneal stromal changes in-vivo after laser in situ keratomileusis with confocal microscopy. Ophthalmology. 2001;108(10):1744-50. Doi: 10.1016/s0161-6420(01)00771-0. PMID: 11581044.
[24] Darwish T, Brahma A, O'Donnell C, Efron N. Subbasal nerve fiber regeneration after LASIK and LASEK assessed by noncontact esthesiometry and in-vivo confocal microscopy: Prospective study. J Cataract Refract Surg. 2007;33(9):1515-21. Doi: 10.1016/j.jcrs.2007.05.023. PMID: 17720064.
[25] Kalteniece A, Ferdousi M, Azmi S, Marshall A, Soran H, Malik RA. Keratocyte density is reduced and related to corneal nerve damage in diabetic neuropathy. Invest Ophthalmol Vis Sci. 2018;59(8):3584-90. Doi: 10.1167/iovs.18-23889. PMID: 30025082.

PARTICULARS OF CONTRIBUTORS:
1. Junior Clinical Fellow, Department of Ophthalmology, Wrexham Maelor Hospital, Wales, United Kingdom.
2. Professor, Department of Pharmacology, Sir Seewoosagur Ramgoolam Medical College, Belle Rive, Mauritius.
3. Junior Doctor, Department of Medicine, Sir Seewoosagur Ramgoolam Medical College, Belle Rive, Mauritius.
4. Director, Department of Cardiology, Cardiac Centre, Sir Seewoosagur Ramgoolam National Hospital (SSRN), Pamplemousses, Mauritius.

NAME, ADDRESS, E-MAIL ID OF THE CORRESPONDING AUTHOR:
Dr. Indrajit Banerjee,
Professor, Department of Pharmacology, Sir Seewoosagur Ramgoolam Medical College, Belle Rive, Mauritius.
E-mail: indrajit18@gmail.com

PLAGIARISM CHECKING METHODS: [Jain H et al.]
- Plagiarism X-checker: Dec 02, 2023
- Manual Googling: Jan 19, 2024
- iThenticate Software: Feb 07, 2024 (6%)

ETYMOLOGY: Author Origin

EMENDATIONS: 6

AUTHOR DECLARATION:
- Financial or Other Competing Interests: None
- Was Ethics Committee Approval obtained for this study? Yes
- Was informed consent obtained from the subjects involved in the study? Yes
- For any images presented appropriate consent has been obtained from the subjects. Yes

Date of Submission: **Nov 28, 2023**
Date of Peer Review: **Jan 05, 2024**
Date of Acceptance: **Feb 09, 2024**
Date of Publishing: **Apr 01, 2024**